Hindawi Publishing Corporation
International Journal of Photoenergy
Volume 2012, Article ID 857345, 7 pages
doi:10.1155/2012/857345

Research Article

Enhanced Hydrogen Production over C-Doped CdO Photocatalyst in Na_2S/Na_2SO_3 Solution under Visible Light Irradiation

Quan Gu, Huaqiang Zhuang, Jinlin Long, Xiaohan An, Huan Lin, Huaxiang Lin, and Xuxu Wang

State Key Laboratory Breeding Base of Photocatalysis, Research Institute of Photocatalysis, Fuzhou University, Fuzhou 350002, China

Correspondence should be addressed to Jinlin Long, jllong@fzu.edu.cn and Xuxu Wang, xwang@fzu.edu.cn

Received 6 December 2011; Revised 12 February 2012; Accepted 13 February 2012

Academic Editor: Weifeng Yao

The C-doped CdO photocatalysts were simply prepared by high-temperature solid-state process. The as-prepared photocatalysts were characterized by X-ray powder diffraction (XRD), diffuse reflectance spectroscopy (UV-Vis DRS), scanning electron microscopy (SEM) and X-ray photoelectron spectroscopy (XPS). The results demonstrated that the carbon was doped into CdO, resulting in the red-shift of the optical absorption of CdO. The photocatalytic behavior of CdO and C-doped CdO was evaluated under the visible light irradiation by using the photocatalytic hydrogen evolution as a model reaction. The C-doped CdO photocatalysts had higher photocatalytic activity over parent CdO under visible light irradiation. The results indicated that the H_2 production was due to the existence of CdS and the enhancement of visible light photocatalytic activity of H_2 production was originated from the doping of carbon into the CdO lattice. The probably reaction mechanism was also discussed and proposed.

1. Introduction

Production of hydrogen, through which a green and potential energy can be obtained, has been deemed to be an alternative to generation energy owing to its own merits such as renewability, environmental friendliness, and high energy capacity. Therefore, numerous studies on photocatalytic H_2 production and a series of semiconductor photocatalysts include metal oxides, nitride, titanates, and niobates [1–6] where high photocatalytic activities for H_2 production have been reported. Unfortunately, these photocatalysts can only work under UV light irradiation. It is essential to develop novel visible light responsive photocatalysts and modification techniques for tuning the photoactivity of UV active photocatalysts into the visible-light region.

Ions doping is one of the most effective ways for modifying the semiconductor photocatalysts to enhance the photoactivity of hydrogen production and to obtain the visible light responsive photocatalysts [7]. Compared with mental doping, the nonmetal doping shifts the valence band edge upward and thus narrows the band gap of the semiconductor. Currently, various nonmetal-doped photocatalysts, such as C-, N-, and S-doped TiO_2[8–10], N-doped ZrO_2 [11], and C-, N-doped In_2O_3 [12, 13], and C-doped Nb_2O_5 [14], have been reported to show enhanced photocatalytic activities for water splitting under visible-light irradiation compared with the undoped samples. Carbon has been considered to be one of the most promising dopants, and C-doped materials were widely investigated in recent years. As the most qualified C-doped materials, C-doped TiO_2 has showed much higher photoactivity for hydrogen production than pure TiO_2 [10, 15]. Jia et al. [16] prepared C-doped $LaCoO_3$ by microorganism chelate method using Bacillus licheniformis R08 biomass as a chelating agent. The photocatalysis tests showed that C-doped $LaCoO_3$ had more obvious advantages in harvesting the visible-light than pure $LaCoO_3$. Sun et al. [12] reported that C-doped In_2O_3 showed highly enhanced photoelectrochemical activity under ultraviolet and visible light irradiation compared with undoped In_2O_3. Guo et al. [17] synthesized C-doped $Zn_3(OH)_2V_2O_7$ nanorods with higher photoactivity than ZnO via a one-step method involving a hydrothermal process in the presence of polyethylene glycol and ethylenediamine tetraacetic acid. Cadmium oxide as a narrow band-gap semiconductor, with specific optical

and electrical properties, has been widely used specifically in the field of optoelectronic devices including solar cells, transparent electrodes, and sensors [18–21]. However, to the best of our knowledge, little work has been attempted to present the photocatalytic property of nonmetal-doped CdO photocatalysts due to special band structure [22].

In the present work, the bulk CdO and C-doped CdO photocatalysts were prepared by the high-temperature solid state process, and their photocatalytic activities for hydrogen evolution from sodium sulfide/sodium sulfite aqueous solution were then compared under visible light irradiation. The results indicated that the photocatalytic activity of the C-doped CdO was higher than that of pure CdO. In addition, these as-prepared C-doped CdO photocatalysts were characterized by X-ray powder diffraction (XRD), diffuse reflectance spectroscopy (UV-Vis DRS), infrared spectroscopy (IR), scanning electron microscopy (SEM), and X-ray photoelectron spectroscopy (XPS). The enhancement of photocatalytic activity for C-doped CdO was discussed, and the probably reaction mechanism was also discussed and proposed.

2. Experimental

2.1. Reagents and Materials. Cadmium sulfate, 8/3-hydrate ($CdSO_4 \cdot 8/3H_2O$, AR grade), cadmium oxide (AR grade), and sodium sulfide (AR grade) were purchased from Aladdin Company. Graphite powder (SR grade) and a sodium sulfite anhydrous (AR grade) were obtained from Sinopharm chemical reagent Co. Ltd. All of the reagents were used without any further purification.

2.2. Preparation of Samples. The samples were prepared by the high-temperature solid state process. For a typical experiment, 3.0 g of $CdSO_4 \cdot 8/3H_2O$ was added in 50 mL of H_2O with constant stirring to obtain the cadmium sulfate solution, and then 1 g of graphite powder was added under vigorously magnetic stirring at room temperature. Stirring of the pravious suspension was continued for 1 hour at the same temperature until the graphite powder was dispersed uniformly in the cadmium sulfate solution. The well-distributed suspension was heated at 120°C on oil bath to evaporate the water, thus the black solid was obtained. The solid was grinded and then calcined on muffle furnace at desired temperature for 10 h.

2.3. Characterization of Samples. The X-ray powder diffraction (XRD) measurements were performed on a Bruker D8 Advance X-ray diffractometer using Cu Kα_1 radiation (λ = 1.5406 Å). The accelerating voltage and the applied current were 40 kV and 40 mA, respectively. The UV-Vis diffuse reflectance spectra were recorded on a Varian Cary 500 Scan UV-Vis-NIR spectrometer with $BaSO_4$ as a reference sample. X-ray photoelectron spectroscopy analysis was conducted on an ESCALAB 250 photoelection spectroscopy (Thermo Fisher Scientific) at 3.0×10^{-10} mbar using Al Kα X-ray beam (15 kv 200 W 500 μm pass energy = 20 eV). All binding energies were referenced to the C 1s peak at 284.6 eV of surface adventitious carbon. The morphologies of the samples were investigated by scanning electron microscopy (SEM) (XL30ESEM, Philips).

2.4. Photocatalytic Activity Measurements. The photocatalytic activities of the samples for hydrogen evolution under visible light irradiation were studied. The photocatalytic H_2 evolution reaction was performed in a closed gas-recirculation system equipped with a side-irradiation Pyrex reaction vessel. 0.4 g of the catalyst was suspended in 400 mL of water containing 3.12 g sodium sulfide and 1.0 g sodium sulfite anhydrous by a magnetic stirrer in Pyrex reaction vessel. The pravious suspension was evacuated 50 min to remove air prior to irradiation under a 300 w xenon lamp with a cutoff filter ($\lambda > 420$ nm). The evolved hydrogen gas was circulated with a gas pump and quantified by gas chromatography (Shimadzu GC-8A, TCD, Ar carrier).

3. Results and Discussion

3.1. XRD Measurement. Figure 1(a) shows the XRD patterns of all samples. For the pure CdO, the peaks associated with planes (111), (200), (220), (311), and (222) are observed, and all XRD peaks can be indexed to CdO (JCPDS 65-2908). When the mixture powders are annealed at 700°C for 10 h, the peaks due to CdO and $Cd_3O_2SO_4$ are observed as shown in Figure 1(a) curve b. The XRD results of samples obtained at above 700°C indicated that the C-doped CdO maintained a cubic structure of CdO. Figure 1(b) is an enlargement of the (111) plane of all samples. As we can see, compared with parent CdO, the peak position of the (111) plane of C-doped CdO is shifted slightly toward lower 2θ value, demonstrating the distortion of the crystal lattice of doped CdO by the carbon dopant. Interestingly, the intensity ratio of (111) and (200) plane is smaller than that of pure CdO and decreased with the increase of preparation temperature. Generally, the preferred orientation could destroy the randomness of plane orientation and the normal relative intensity of plane. So, it seems that the samples synthesized at high temperature grow preferentially along (111) plane orientation.

3.2. UV-Vis DRS Measurement. Figure 2 shows the diffuse reflectance spectra of the prepared samples. It is clearly observed that a strong absorption band exists in the range of 200–600 nm for parent CdO and an optical absorption edge of pure CdO is at 620 nm. The parent CdO exhibits a weak adsorption at the range of 620–800 nm, which may be due to the adsorbed C species as indicated in XPS results. Therefore, the corresponding value of the band-gap energy is about 2.2 eV, which is smaller about 0.1 eV than that of the reference value (2.3 eV) of the band-gap energy [20]. It may be due to the effect of CdO crystallites diameter on optical absorption and difference of synthesis procedures [19, 20, 23]. Compared with parent CdO, the C-doped CdO adsorbed the light at the range of 200–800 nm. The broad absorption band of C-doped CdO is probably associated with the formation of impurity states in the band gap by the partial substitution of O with C in the crystal lattice of CdO.

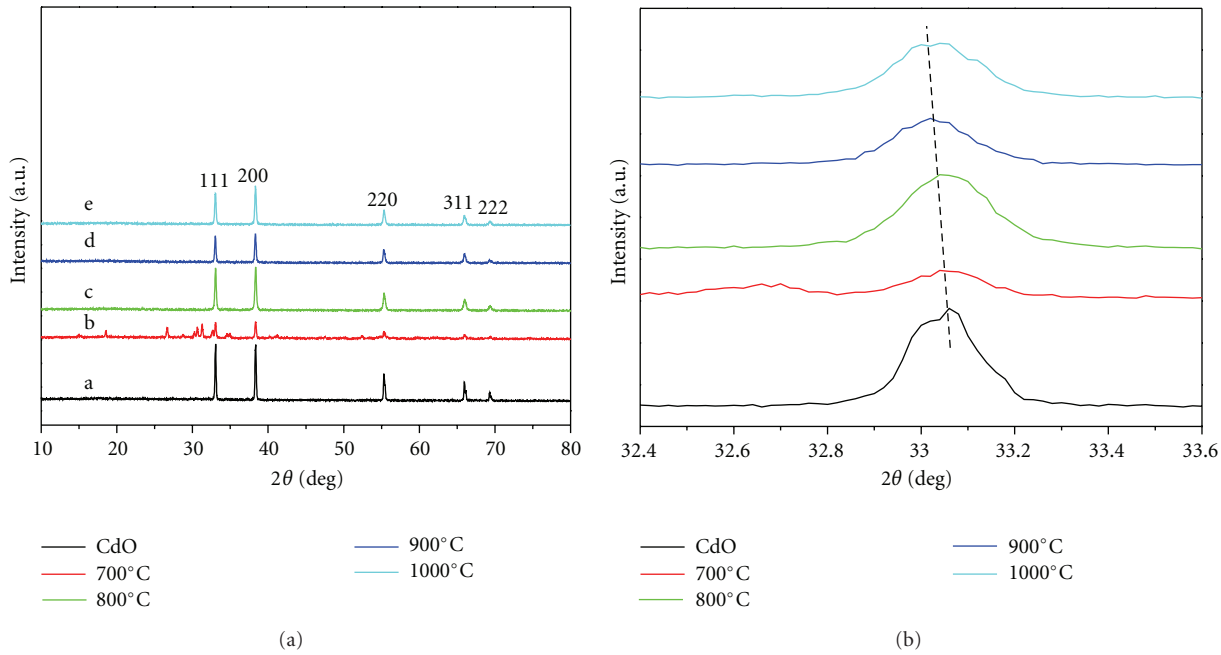

Figure 1: XRD patterns of samples.

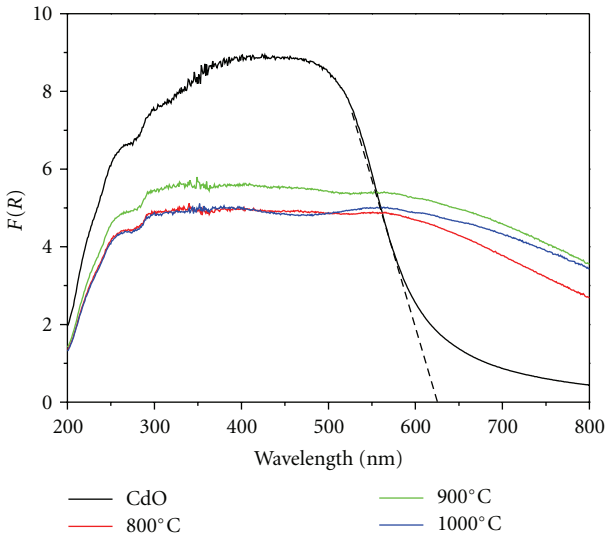

Figure 2: UV-Vis diffuse reflectance spectra of pure CdO and C-doped CdO samples prepared under different temperatures.

Therefore, the results indicated that C-doping into the CdO lattice leads to the red-shift of the optical absorption for the C-doped CdO.

3.3. SEM and IR Studies. The scanning electron microscopy (SEM) image of C-doped CdO sample prepared by the high temperature calcinations is shown in Figure 3(a). It shows that the as-prepared C-doped CdO sample form very large massive particles and the average size of block is about 10 μm, which is caused by high-temperature calcinations. When samples are calcined at high temperature, crystals grow along a plane into large particles and the as-prepared samples have good crystallinity, which can also be observed in the XRD patterns.

The infrared spectra changes of CdO created by C doping are presented in Figure 3(b). The IR spectrum of the CdO shows seven bands centered at 3433, 1634, 1401, 983, 859, 684 and, 591 cm^{-1}. The broad band near 3433 cm^{-1} and the weak band at 1634 cm^{-1} are assigned to OH-stretching vibrations and deformative vibration of adsorbed H_2O, respectively. According to [19, 24], CdO phase is characterized by an intense and very broad IR band with poor resolved shoulders at 1400, 1000, and 580 cm^{-1}. Therefore, we believe that the bands at 1401, 983, 859, 684, and 591 cm^{-1} are assigned to the CdO phase. After C-doping, a new band at 1109 cm^{-1} is formed in IR spectrum of samples compared with the IR spectrum of pure CdO, which is thought to be related to the C-Cd stretching.

3.4. XPS Analysis. To investigate the chemical state of the possible dopant incorporated into CdO and the effect of dopant on chemical states of other elements, pure CdO and C-doped CdO samples were characterized by XPS, as shown in Figure 4.

Figure 4(a) presents the C1s XPS spectra of CdO and C-doped CdO. The C1s XPS spectrum of pure CdO shows two peaks at 284.6 and 289.4 eV and a very small peak at 287.0 eV (Negligible). These three C 1s peaks are also observed in C 1s XPS spectra of C-CdO. The peak with a binding energy of 284.6 eV is assigned to surface adventitious carbon. The peak at 289.4 eV can be assigned to the chemisorbed carbon species on the surface of CdO [25]. The new peak with the binding energy at 282.5 eV is observed in the C

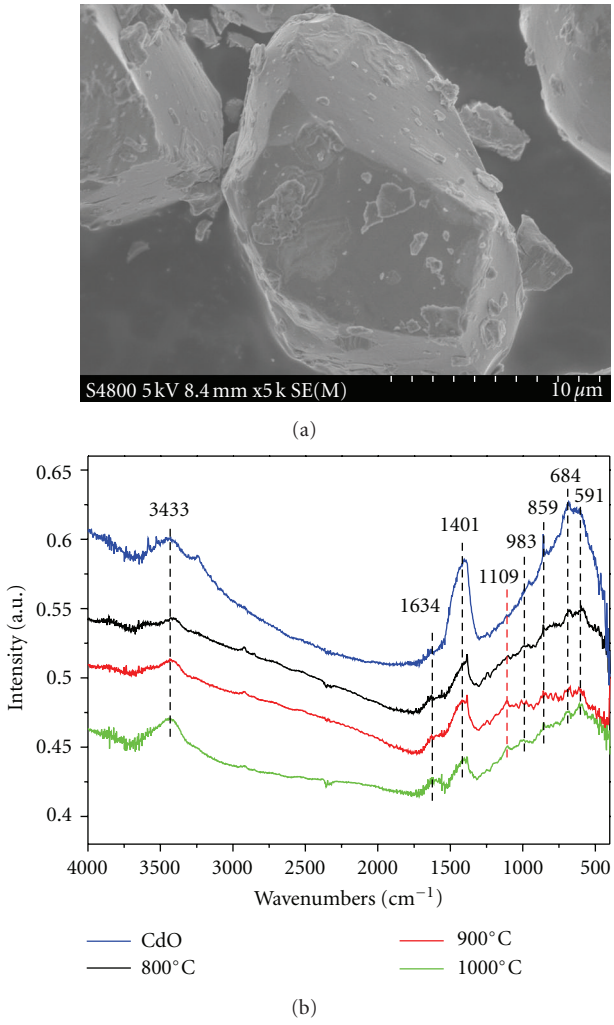

Figure 3: (a) SEM image of the C-doped CdO samples synthesized at 1000°C. (b) The infrared spectra changes of CdO induced by C doping.

1s XPS spectrum of C-doped CdO, which suggests that a new chemical state of carbon species is formed during the doping process. Jia et al. [16] assigned the peak at 282.8 eV to Co–C in C-doped $LaCoO_3$. The C1s peak around 282 eV was ascribed to the existence of O–Ti–C bonds by Wang [25]. Jang et al. [26] demonstrated that the broad peak around 280–284 eV could be assigned to carbon interacting with Zn through Zn–C bond formation. The Cd 3d3/2 XPS spectra of parent CdO and C-doped CdO are shown in Figure 4(b). The Cd 3d3/2 peak at 411.8 of parent CdO can be assigned to lattice Cd atoms and the peak at 410.2 eV may be originated from the interaction between CdO and chemisorbed carbon species, which is in parallel with the result of C1s XPS spectra. The Cd 3d3/2 XPS spectra of C-doped CdO show two peaks at 410.2 and 411.8 eV and the intensity ratio of 410.2 and 411.8 eV increased with the increase of preparation temperature. We consider that the peak assigned to C–Cd species is overlapped with the peak originated from chemisorbed carbon species. According to these results, it can be concluded that C is doped into the CdO lattice.

3.5. Visible Light Photocatalytic Activity for H_2 Production. The photocatalytic activities for H_2 evolution of CdO and C-doped CdO synthesized at different temperatures (800°C, 900°C, and 1000°C) under the visible light irradiation are shown in Figure 5. It can be seen that both the CdO and C-doped CdO could photoinduce production of H_2 and the amounts of H_2 evolved for all samples increase with the irradiation time. The turnover numbers of CdO and C-doped CdO prepared at 800°C, 900°C, and 1000°C, which was calculated from the molar amount of H_2 and the molar amount of photocatalysts [27], are 1.4, 3.1, 3.6, and 7.5, respectively. These values suggest that the reaction proceeded photocatalytically. The pure CdO displays a low activity for H_2 evolution from the aqueous solutions containing Na_2S/Na_2SO_3 as sacrificial reagents. The C-doped CdO samples prepared at different temperatures have higher photocatalytic activity than pure CdO under the visible light irradiation by using Na_2S/Na_2SO_3 as sacrificial reagents, and the photocatalytic H_2 evolution activity for these samples increased in the order of CdO < 800°C < 900°C < 1000°C. The results demonstrated that the C-doped CdO could significantly improve the photocatalytic H_2 production activity under visible light irradiation by carbon doping. In addition, it can be seen that the amount of produced H_2 over the C-CdO-1000 increases slowly with irradiation time in 5 h; then the H_2 production rate increases after 5 h irradiation.

In general, to facilitate the reduction of H_2O by photoexcited electrons, the match of conduction band of semiconductor photocatalyst with the reduction potential of H^+/H_2 (0 V versus NHE) is very important. In other words, the bottom level of the conduction band of photocatalyst has to be more negative than the reduction potential of H^+/H_2 (0 V versus NHE). However, the energy level of conduction band edge for cadmium oxide is −4.61 eV versus Absolute Vacuum Scale (AVS) [22]; according to $E_{(NHE)} = E_{(AVS)} - 4.50$, the E_{NHE} of cadmium oxide is located at 0.11 eV, which is positive than the reduction potential of H^+/H_2. Hence, theoretically, the photogenerated electrons in the conduction band of CdO cannot reduce the H^+ in the aqueous solution in the absence of sacrificial reagents. Interestingly, the addition of sodium sulfide and cadmium sulfate into solution leads to the production of hydrogen from water under the visible light irradiation. It is well known that electronic structures of cadmium sulfide match well with the redox potential of water into hydrogen. So, on the basis of experimental results, we hypothesized that cadmium sulfide maybe formed on surface of CdO during the visible light irradiation and photogenerated electrons in the conduction band of CdS could reduce the H^+ into H_2. This is also the reason why the photocatalytic reactivity of C-CdO-1000 increases after 5 h irradiation. After the formation of CdS on the surface of C-CdO-1000, the interactions between CdS and C-doped CdO promote the activity. To testify the formation of CdS on the surface of CdO during the

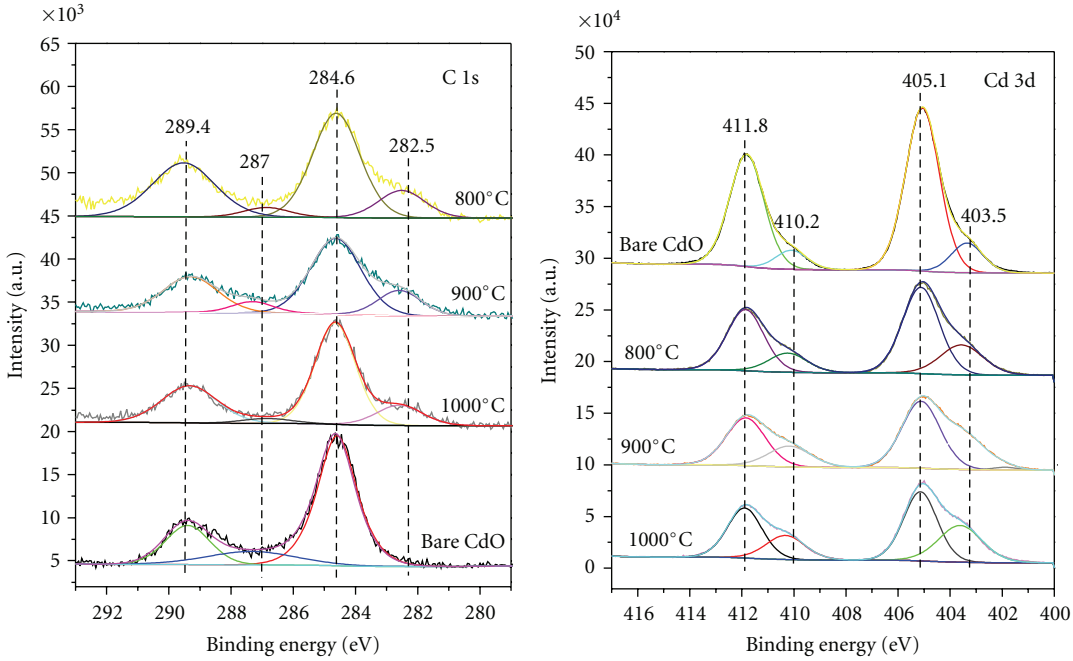

Figure 4: XPS spectra of the pure CdO and C-doped CdO samples prepared under different temperatures.

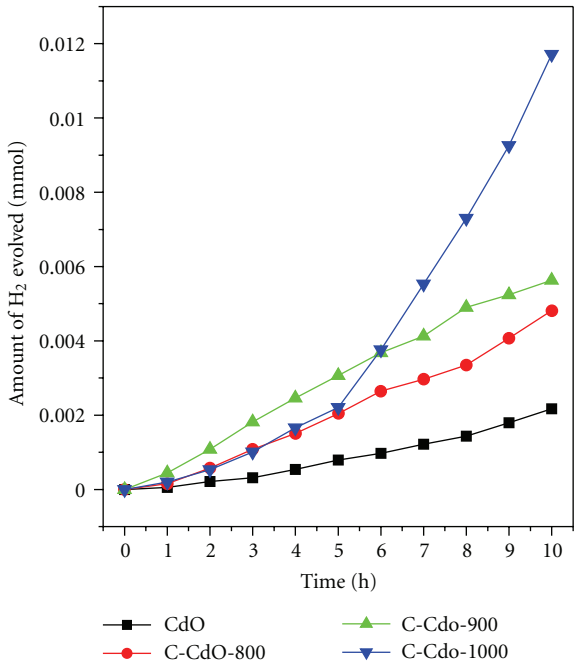

Figure 5: Photocatalytic hydrogen amount as a function of irradiation time.

photoreaction, the S 2p XPS spectrum of CdO after reaction are recorded and shown in Figure 6(a). Two peaks at 161.5 and 162.6 eV are observed, which are consistent with the reported values of CdS in the literatures [28]. It is confirmed that CdS were formed on the surface of CdO. However, no CdS phase is observed after irradiation in XRD pattern, as shown in Figure 6(b). It indicates that the CdS formed on the surface of CdO is amorphous and/or its content is lower than the detect limit of XRD apparatus.

In our photocatalytic system, the CdO and the CdS formed by photocorrosion are activated by visible light simultaneously. The photogenerated h^+ would transferred from the valence band of CdO to that of CdS, while the photogenerated e^- on the conduction band of CdS would be reduce the H_2O to H_2 and/or inject to the conduction band of CdO. Similar to case of other nonmetal-doped catalysts, C doping in CdO causes a valence band upward shift to a higher energy level, which narrows the band gap. It is facilitating to the electron-hole separation. Therefore, the photoactivity of C-doped CdO for hydrogen evolution in Na_2S/Na_2SO_3 solution is higher than that of pure CdO sample under the same reaction conditions. It can be subsequently concluded that the H_2 production is due to the existence of CdS and the enhancement of visible light photocatalytic activity of H_2 production is originated from the C doping into CdO lattice. The proposed reaction mechanism for accelerating the photocatalytic H_2 production process over the C-CdO photocatalysts is demonstrated in Scheme 1.

4. Conclusions

C-doped CdO photocatalysts with visible light response are prepared by high-temperature solid state process. The experiment characterization results such as XRD, UV-Vis DRS, IR, and XPS indicate that C is doped into the CdO lattice. The photocatalytic hydrogen production activities of as-prepared photocatalysts are studied under the visible light

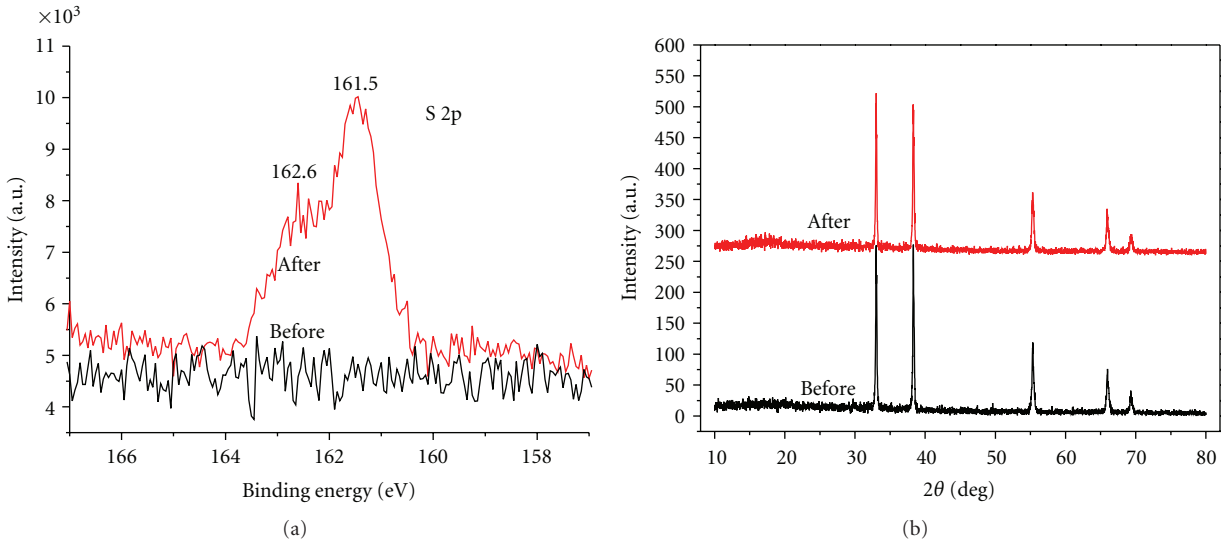

Figure 6: (a) XPS spectra of the C-doped CdO before and after photocatalytic H_2 evolution reaction. (b) XRD patterns of C-doped CdO before and after photocatalytic H_2 evolution reaction.

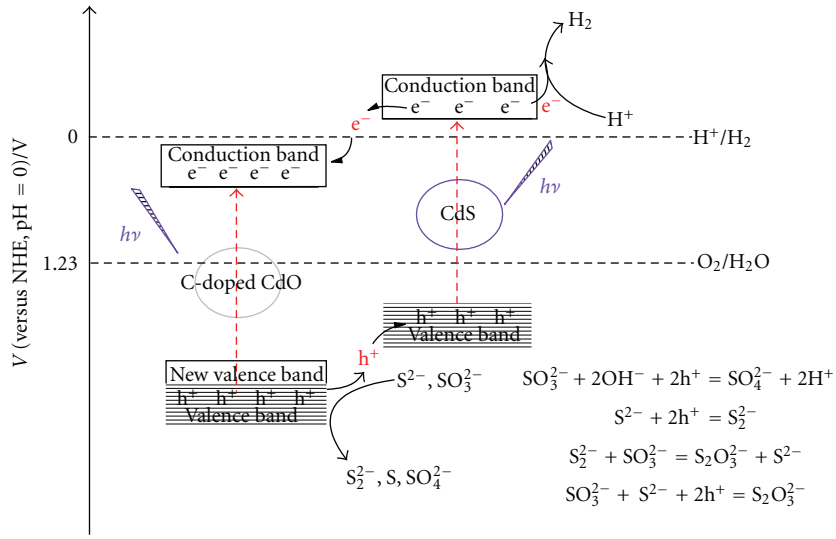

Scheme 1: Proposed photocatalytic hydrogen evolution process over the C-doped CdO.

irradiation. The C-doped CdO photocatalysts exhibit higher photoactivity for hydrogen production over undoped CdO under visible light irradiation by using the Na_2S/Na_2SO_3 as sacrificial reagents, which indicated that the formation of CdS is an important factor for the hydrogen production and C doping into CdO lattice results in the enhancement of photocatalytic hydrogen production activity of CdO.

Acknowledgments

This work was financially supported by the NSFC (Grants Nos. 21003021, 20873022, and 21173044), the National High Tech R&D Program of China (863 Program, 2008AA06Z326), Program for Changjiang Scholars and Innovative Research Team in University (PCSIRT0818), the Natural Science Foundation of Fujian Province of China (2010J05024), and the Science and Technology Project of Education Office of Fujian Province of China (JK2010002).

References

[1] Y. Wang, Z. Zhang, Y. Zhu et al., "Nanostructured VO_2 photocatalysts for hydrogen production," *ACS Nano*, vol. 2, no. 7, pp. 1492–1496, 2008.

[2] G. N. Schrauzer and T. D. Guth, "Photolysis of water and photoreduction of nitrogen on titanium dioxide," *Journal of the American Chemical Society*, vol. 99, no. 22, pp. 7189–7193, 1977.

[3] X. Chen, T. Yu, X. Fan et al., "Enhanced activity of mesoporous Nb_2O_5 for photocatalytic hydrogen production," *Applied Surface Science*, vol. 253, no. 20, pp. 8500–8506, 2007.

[4] K. Maeda, N. Saito, D. Lu, Y. Inoue, and K. Domen, "Photocatalytic properties of RuO_2-loaded β-Ge_3N_4 for overall water splitting," *The Journal of Physical Chemistry C*, vol. 111, no. 12, pp. 4749–4755, 2007.

[5] J. S. Jang, S. H. Choi, D. H. Kim, J. W. Jang, K. S. Lee, and J. S. Lee, "Enhanced photocatalytic hydrogen production from water-methanol solution by nickel intercalated into titanate nanotube," *The Journal of Physical Chemistry C*, vol. 113, no. 20, pp. 8990–8996, 2009.

[6] K. Domen, A. Kudo, M. Shibata, A. Tanaka, K. I. Maruya, and T. Onishi, "Novel photocatalysts, ion-exchanged $K_4Nb_6O_{17}$, with a layer structure," *Journal of the Chemical Society*, no. 23, pp. 1706–1707, 1986.

[7] X. Chen, S. Shen, L. Guo, and S. S. Mao, "Semiconductor-based photocatalytic hydrogen generation," *Chemical Reviews*, vol. 110, no. 11, pp. 6503–6570, 2010.

[8] L. Randeniya, A. Murphy, and I. Plumb, "A study of S-doped TiO_2 for photoelectrochemical hydrogen generation from water," *Journal of Materials Science*, vol. 43, no. 4, pp. 1389–1399, 2008.

[9] J. Yuan, M. Chen, J. Shi, and W. Shangguan, "Preparations and photocatalytic hydrogen evolution of N-doped TiO_2 from urea and titanium tetrachloride," *International Journal of Hydrogen Energy*, vol. 31, no. 10, pp. 1326–1331, 2006.

[10] S. U. M. Khan, M. Al-Shahry, and W. B. Ingler, "Efficient photochemical water splitting by a chemically modified n-TiO_2," *Science*, vol. 297, no. 5590, pp. 2243–2245, 2002.

[11] T. Mishima, M. Matsuda, and M. Miyake, "Visible-light photocatalytic properties and electronic structure of Zr-based oxynitride, Zr_2ON_2, derived from nitridation of ZrO_2," *Applied Catalysis A*, vol. 324, no. 1-2, pp. 77–82, 2007.

[12] Y. Sun, C. J. Murphy, K. R. Reyes-Gil, E. A. Reyes-Garcia, J. P. Lilly, and D. Raftery, "Carbon-doped In_2O_3 films for photoelectrochemical hydrogen production," *International Journal of Hydrogen Energy*, vol. 33, no. 21, pp. 5967–5974, 2008.

[13] K. R. Reyes-Gil, E. A. Reyes-García, and D. Raftery, "Nitrogen-doped In_2O_3 thin film electrodes for photocatalytic water splitting," *The Journal of Physical Chemistry C*, vol. 111, no. 39, pp. 14579–14588, 2007.

[14] S. Ge, H. Jia, H. Zhao, Z. Zheng, and L. Zhang, "First observation of visible light photocatalytic activity of carbon modified Nb_2O_5 nanostructures," *Journal of Materials Chemistry*, vol. 20, no. 15, pp. 3052–3058, 2010.

[15] C. Xu, Y. A. Shaban, W. B. Ingler Jr, and S. U. M. Khan, "Nanotube enhanced photoresponse of carbon modified (CM)-n-TiO_2 for efficient water splitting," *Solar Energy Materials and Solar Cells*, vol. 91, no. 10, pp. 938–943, 2007.

[16] L. Jia, J. Li, W. Fang, H. Song, Q. Li, and Y. Tang, "Visible-light-induced photocatalyst based on C-doped $LaCoO_3$ synthesized by novel microorganism chelate method," *Catalysis Communications*, vol. 10, no. 8, pp. 1230–1234, 2009.

[17] H. Guo, J. Chen, W. Weng, and S. Li, "Hydrothermal synthesis of C-doped $Zn_3(OH)_2V_2O_7$ nanorods and their photocatalytic properties under visible light illumination," *Applied Surface Science*, vol. 257, no. 9, pp. 3920–3923, 2011.

[18] Q. Chang, C. Chang, X. Zhang et al., "Enhanced optical limiting properties in suspensions of CdO nanowires," *Optics Communications*, vol. 274, no. 1, pp. 201–205, 2007.

[19] N. C. S. Selvam, R. T. Kumar, K. Yogeenth, L. J. Kennedy, G. Sekaran, and J. J. Vijaya, "Simple and rapid synthesis of Cadmium Oxide (CdO) nanospheres by a microwave-assisted combustion method," *Powder Technology*, vol. 211, no. 2-3, pp. 250–255, 2011.

[20] O. Vigil, F. Cruz, A. Morales-Acevedo, G. Contreras-Puente, L. Vaillant, and G. Santana, "Structural and optical properties of annealed CdO thin films prepared by spray pyrolysis," *Materials Chemistry and Physics*, vol. 68, no. 1–3, pp. 249–252, 2001.

[21] C. H. Bhosale, A. V. Kambale, A. V. Kokate, and K. Y. Rajpure, "Structural, optical and electrical properties of chemically sprayed CdO thin films," *Materials Science and Engineering B*, vol. 122, no. 1, pp. 67–71, 2005.

[22] X. Yong and M. A. A. Schoonen, "The absolute energy positions of conduction and valence bands of selected semiconducting minerals," *American Mineralogist*, vol. 85, no. 3-4, pp. 543–556, 2000.

[23] A. Gulino, G. Compagnini, and A. A. Scalisi, "Large third-order nonlinear optical properties of cadmium oxide thin films," *Chemistry of Materials*, vol. 15, no. 17, pp. 3332–3336, 2003.

[24] A. Askarinejad and A. Morsali, "Syntheses and characterization of $CdCO_3$ and CdO nanoparticles by using a sonochemical method," *Materials Letters*, vol. 62, no. 3, pp. 478–482, 2008.

[25] H. Wang, Z. Wu, and Y. Liu, "A simple two-step template approach for preparing carbon-doped mesoporous TiO_2 hollow microspheres," *The Journal of Physical Chemistry C*, vol. 113, no. 30, pp. 13317–13324, 2009.

[26] J. S. Jang, C.-J. Yu, S. H. Choi, S. M. Ji, E. S. Kim, and J. S. Lee, "Topotactic synthesis of mesoporous ZnS and ZnO nanoplates and their photocatalytic activity," *Journal of Catalysis*, vol. 254, no. 1, pp. 144–155, 2008.

[27] A. Kudo, I. Tsuji, and H. Kato, "$AgInZn_7S_9$ solid solution photocatalyst for H_2 evolution from aqueous solutions under visible light irradiation," *Chemical Communications*, no. 17, pp. 1958–1959, 2002.

[28] S. Rengaraj, S. Venkataraj, S. H. Jee et al., "Cauliflower-like CdS microspheres composed of nanocrystals and their physicochemical properties," *Langmuir*, vol. 27, no. 1, pp. 352–358, 2011.